Journal of Crystal Growth 127 (1993) 296–301
North-Holland

JOURNAL OF CRYSTAL GROWTH

# CdTe/InSb/α-Sn heterostructures grown by molecular beam epitaxy

Nathaniel Libatique [a], Atsushi Sasaki [a], Dukuraku Choi [a], Shinichi Wada [a], Alok C. Rastogi [a,1], Morihiko Kimata [a], Kazuhiko Kaneko [b] and Masaki Takashima [c]

[a] *Electrical Engineering Department, Waseda University, Shinjuku-ku, Tokyo 169, Japan*
[b] *North Shore College, Atsugi, Kanagawa 243, Japan*
[c] *Mitsubishi Kasei, Midori-Ku, Yokohama 227, Japan*

MBE-grown CdTe/InSb/CdTe single quantum wells were characterized by TEM, FTIR and photoconduction. Even in the presence of In, Te related compounds and CdTe buffer-width dependent Fabry–Perot interference, a step-like quantum size effect was observed in the SQW FTIR data. The photocurrent peaks are also attributable to quantum well intersubband transitions due to higher subband energy levels. With the improvement of the CdTe/InSb interface in mind, we studied the characteristics of α-Sn layers grown on top of CdTe. TEM pictures show that the propagation of dislocation planes originating from the CdTe buffer layer is stopped at the α-Sn/CdTe heterointerface.

## 1. Introduction

Heterostructures based on InSb/CdTe layers have attracted considerable research attention in recent years, stemming essentially from their near ideal material parameters. Both have matching lattice constants to within 0.05% and compatible coefficients of thermal expansion over a wide (77–600 K) temperature range. Owing to the low effective mass of the electrons, narrow gap InSb has high electron mobility and quantum size effects could occur even in wide wells. These properties are very promising for device applications in low temperature HEMTs and medium wavelength infrared detectors and lasers.

However, formation of InSb/CdTe heterostructures by MBE has been beset with considerable technological problems.

Incompatibility of optimal growth temperatures for InSb ($300 < T_g < 400$°C [1]) and CdTe ($150 < T_g < 220$°C [2]), cross-doping [3], and the formation of In, Te-related compounds at the interfaces [4] are the serious problems encountered in this material system. To alleviate these problems, Williams et al. [5] have used a modified two-step growth method to elevate CdTe growth temperatures to as high as 310°C, Zahn et al. [6] have applied excess cadmium overpressure during CdTe growth to inhibit the undesirable In, Te chemical reaction, Glenn et al. [7] have used separate MBE chambers for the growth of InSb and CdTe to prevent cross contamination, and we [8] attempted to reduce the growth temperature of InSb by reducing the arrival ratio of antimony molecules with respect to indium molecules.

n-Type inversion layers at the surface of bulk crystals or at MBE-grown interfaces have already been reported [9–12]; however, to the best of our knowledge, for this single quantum well material system a two-dimensional electron gas has not yet been observed.

## 2. MBE growth

For the growth, we used a specially designed MBE chamber. A distinguishing feature of this chamber is the cryopanel design which effectively separates the effusion cells from the epilayer growth side with the exception of the narrow orifices placed appropriately to allow the passage

[1] Present address: National Physical Laboratory, New Delhi 110012, India.

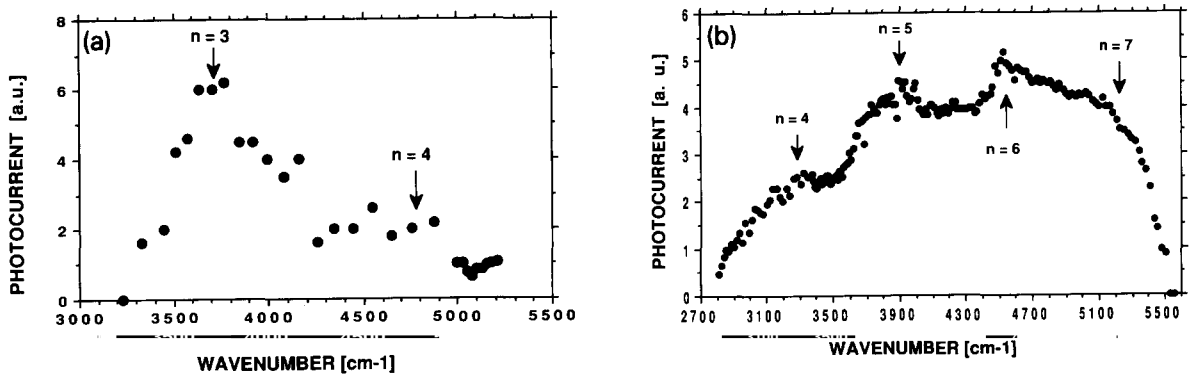


Fig. 1. (a) Photocurrent response of sample A at 133 K, $L_{eff} = 19.4$ nm. (b) Photocurrent response of sample B at 133 K, $L_{eff} = 33$ nm. The numbers denote electron heavy hole intersubband transitions with selection rule $\Delta n = 0$ assumed.

of the incident molecular beams. This design drastically reduces the background tellurium pressure in the vicinity of the substrate while InSb is being deposited.

The pressure of the molecules at the surface of the substrate was observed right after the shutter was closed. The exponential decay time constants for CdTe, In and Sb were less than 2 s.

The two CdTe/InSb/CdTe single quantum wells investigated here were grown on (001) GaAs substrates at the following growth conditions: the growth temperature, growth rate and V/III arrival ratios were 220°C, 0.1 $\mu$m/h and 1.0, respectively, and the growth rate of CdTe was 0.3 $\mu$m/h. Sample A had a 1.1 $\mu$m thick CdTe buffer layer, while sample B had 2.7 $\mu$m.

Quantum states in the SQW structures were investigated by infrared optical absorption and photoconduction measurements. These are greatly facilitated because the underlying GaAs is transparent to the infrared region of interest and the substrate's high resistivity enables direct measurements of photocurrent without shorting the current signal.

As for the α-Sn/CdTe/InSb polytype heterostructures, CdTe and InSb were grown at 220°C and α-Sn was grown at the lower temperature of 70°C. The 13.2°C α-Sn to metallic β-Sn transition temperature can be raised by the stabilization effect [13]. We have already shown before [14] that α-Sn can be grown at higher temperatures if the layers are grown thin.

## 3. Photoconduction and FTIR

Fig. 1 shows the results of the photocurrent measurements conducted at 133 K for the two SQW samples. The peaks are attributed to electron–heavy hole transitions excited by photons impinging on the sample. The broadness of the peaks reveals the effect of quantum well width irregularities over the sample area. Transitions indexed by 1 and 2 do not appear in fig. 1a because the lower subbands are filled in these photoconduction measurements. In fig. 1b, subband levels up to 3 are filled. Calculating with an effective well width of 15 monolayers (19.4381

Table 1
Parameters interpolated at 133 K from published data

| Temperature (K) | Valence band discontinuity (eV) | Split-off band discontinuity (eV) | Band gap (InSb) (eV) | Band gap (CdTe) (eV) | $\Delta_{so}$ (InSb) (eV) | $\Delta_{so}$ (CdTe) (eV) |
|---|---|---|---|---|---|---|
| 133 | 0.88 | 0.74 | 0.22 | 1.59 | 0.95 | 0.81 |
| 293 | 0.84 | 0.66 | 0.17 | 1.50 | 0.98 | 0.80 |

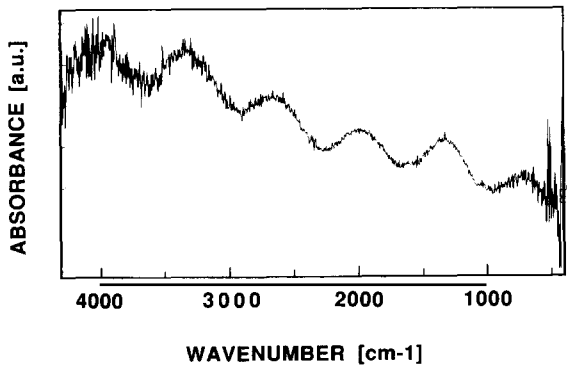


Fig. 2. Fourier transform infrared absorption curve for sample B at room temperature.

nm) for sample A and 23.5 monolayers (33.0448 nm) for sample B, we obtain the transition number assignments shown in the figures. Even with the present uncertainty in the value of the InSb/CdTe valence band discontinuity, recent values ranging from 0.96 eV down to 0.84 eV [15], the resulting difference in calculated emission peaks is only of the order of 10 $cm^{-1}$ which is not enough to change the peak assignments shown.

Table 1 shows the parameters [16–18] used to calculate the subband transitions at 133 K. We used a simple non-parabolic conduction band model with the heavy hole band decoupled from the light hole, split-off and conduction bands according to the method outlined in Bastard and Brum's [19] review article. The field used in the photoconduction experiment was assumed to be small enough to be neglected in the calculations. Exciton effects were also not included, owing to the rather rough resolution of the measurements.

Fig. 2 shows the Fourier transform infrared (FTIR) absorption curve for sample B. The upper curve in fig. 3 shows the measured data after smoothing. The interference (which can be varied by changing the buffer layer thickness) is clearly seen. We assume that below the InSb band edge absorption energy, only the sinusoidal interference predominates. Hence, we can safely estimate the period and amplitude of the sinusoid over this region, as shown in the middle curve in fig. 3, and the step-like response is obtained after dividing out the assumed interfering sinusoid. The same thing cannot be done for sample A because the buffer layer (1.1 $\mu$m) proved to be too thin, therefore the interference period exceeded the onset of the optical absorption threshold.

If we attribute the step edges to electron–heavy hole transitions, then the computed arrows shown in the figure correspond to transitions $n = 1$ to $n = 5$. The $n = 2$ transition does not seem to fall near any observable edge; however, all the other transitions occur near the middle of the step edges, as was expected. The InSb fundamental energy gap coincides with the absorption peak at 1370 $cm^{-1}$, as seen in fig. 3. A possible explanation for the appearance of this peak is the precipitation of InSb islands at the well interfaces.

The verification of the well width is a complicated issue. For sample A, the width is about 20 nm according to flux measurements, and this agrees quite well with the theoretical effective well width used to explain the photocurrent response. But for sample B, if flux measurements are to be followed, the width should be approximately 40 nm, which does not exactly tally with the effective well width used to fit the photoresponse peaks and the FTIR absorption curve.

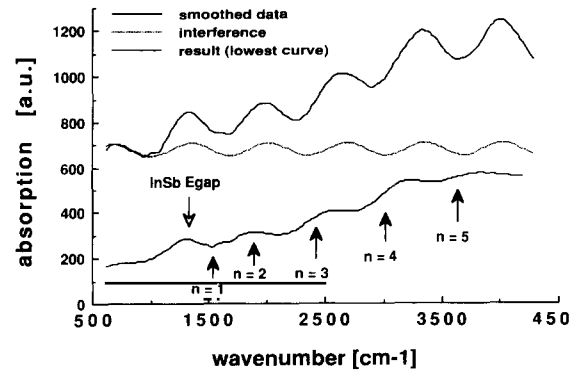


Fig. 3. The smoothed FTIR absorption curve is shown at the top. The Fabry–Perot interference is modelled by the sinusoid whose phase and amplitude are chosen so as to eliminate the first peak in the upper curve, the assumption being that the interference dominates the low energy part of the absorption spectrum (below the $\Gamma_0$ optical threshold of InSb). For easier viewing, the two topmost curves are displaced by 450 arbitrary units and the lowest curve is a 180 times magnification of the real result.

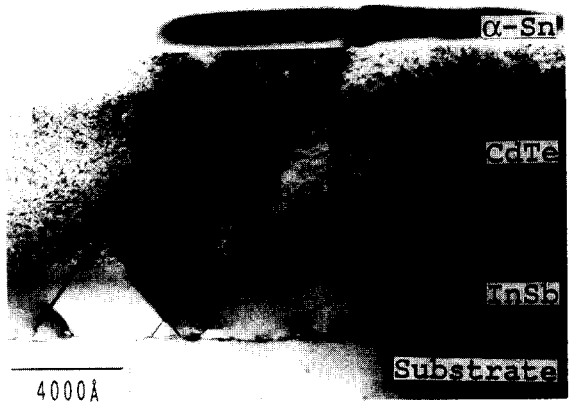


Fig. 4. Transmission electron micrograph of the α-Sn/CdTe/InSb heterostructure. Dislocations starting from the InSb substrate are stopped at the α-Sn/CdTe interface.

## 4. TEM

Some effort was invested into possible ways of improving the CdTe/InSb interface and avoiding the problems due to the formation of In, Te related compounds. For this purpose, we chose α-Sn as a candidate material because of the following properties: it has a good lattice match with CdTe and InSb and it has a zero band gap which makes it suitable as a possible layer located at the SQW interfaces.

In this study, the α-Sn/CdTe/InSb(substrate) polytype heterostructure was investigated using transmission electron micrographs (TEM) and TEM energy dispersive X-ray (TEM EDX) analysis.

Fig. 4 clearly shows the appearance of planar dislocations within the CdTe buffer layer grown on top of the InSb substrate, and they propagate right up to the start of the CdTe/α-Sn heterointerface. No propagation is observed within the thin grey tin layer. The defects which originated from the polar buffer layer are apparently stopped by the onset of the non-polar grey tin layer.

However, we have recently made Raman studies that indicate In, Te related compound formation despite the presence of an α-Sn layer between CdTe and InSb [20]. This result suggests the diffusion of tellurium and indium through the α-Sn stop layer.

A TEM picture of a 200 nm long part of sample A is shown in fig. 5. The irregularity of the InSb well width evident in the figure clearly accounts for the broadness of the photoconductive response peaks. Some clear planar dislocations can also be seen, and this, coupled with the precipitation of indium near the interface, causes


Fig. 5. TEM study of a 200 nm part of the SQW sample A. The irregularity of the quantum well width spacing is plainly seen.


Fig. 6. TEM multiple wave interference picture of the CdTe/InSb(buffer) interface of the polytype heterostructure after bombardment with a 300 keV beam of electrons. Damaged sites appear blacker than the surrounding area. Both sides of the interface were equally bombarded, but the InSb side has relatively little damage.

degradation in the expected high carrier mobility. In fact, Van der Pauw measurements showed mobilities in the order of $10^3$ $cm^2/V \cdot s$.

During the TEM EDX measurement, 300 keV electrons were used to irradiate the polytype heterostructure. Fig. 6 shows a small part of the CdTe/InSb interface after irradiation. The dark spots are caused by the evaporation of tellurium atoms due to the electron bombardment. The InSb layer side shows significantly less damage, indicating that comparatively, RHEED measurements during MBE growth (though electron energies are considerably less here, about 20 keV) have less deleterious effects during InSb growth as compared to CdTe layer growth. TEM EDX graphs (fig. 7) of a particular spot in the crystal show quantitatively the decrease in tellurium concentration as compared to cadmium after the bombardment.

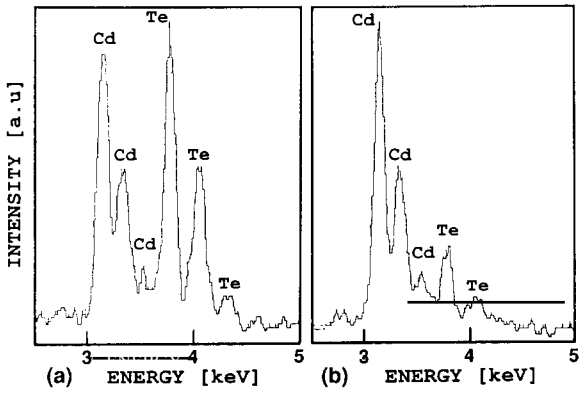


Fig. 7. TEM EDX graphs of a particular region in the CdTe layer before and after the 300 keV electron bombardment. The evaporation of tellurium is seen by the decrease in intensity of the tellurium peaks.

## 5. Summary

In summary, we have grown CdTe/InSb/CdTe single quantum wells on (001) GaAs substrates. Irregularities in well width seen in the transmission electron micrographs account for the broad photocurrent peaks and the low mobility is due to the planar dislocations and the oft-reported for-

mation of In, Te related compounds. However, optical transitions attributable to the presence of a two-dimensional electron gas are clearly seen in the FTIR and photoconduction measurements, probably for the first time.

Seeking to improve the SQW interfaces, we attempted the growth of polytype α-Sn/CdTe/InSb heterostructures. Planar dislocations propagating through the CdTe buffer layer were suppressed by a thin α-Sn layer.

## Acknowledgements

One of the authors would like to thank JASCAA (Japan Solidarity Committee for Asian Alumni) for a study grant that made his participation in this research possible, and Fr. Dan McNamara, Physics Chairperson of the Ateneo de Manila University, for his continued encouragement and support.

## References

[1] M. Yano, T. Takase and M. Kimata, Phys. Status Solidi (a) 54 (1979) 707.
[2] R.F.C. Farrow, G.R. Jones, G.M. Williams and I.M. Young, Appl. Phys. Letters 39 (1981) 954.
[3] G.M. Williams, C.R. Whitehouse, T.R. Martin, N.G. Chew, A.G. Cullis, T. Ashley, D.E. Sykes, K. Mackey and R.H. Williams, J. Appl. Phys. 63 (1988) 1526.
[4] K.J. Mackey, D.R.T. Zahn, P.M.G. Allen, R.H. Williams, W. Richter and R.S. Williams, J. Vacuum Sci. Technol. B 5 (1987) 1233.
[5] G.M. Williams, C.R. Whitehouse, N.G. Chew, C.W. Blackmore and A.G. Cullis, J. Vacuum Sci. Technol. B 3 (1985) 704.
[6] D.R.T. Zahn, R.H. Williams, T.D. Golding, J.H. Dinan, K.J. Mackey, J. Geurts and W. Richter, Appl. Phys. Letters 53 (1988) 2409.
[7] J.L. Glenn, Jr., Sungki O, L.A. Kolodziejski, R.L. Gunshor, M. Kobayashi, D. Li, O. Otsuka, M. Haggerott, N. Pelekanos and A.V. Nurmikko, J. Vacuum Sci. Technol. B 7 (1989) 249.
[8] M. Kimata, A. Ryoji and T. Aoki, J. Crystal Growth 81 (1987) 508.
[9] N. Kotera, Y. Katayama and K. Komatsubara, Phys. Rev. B 5 (1972) 3065.
[10] A. Darr and J.P. Kotthaus, Surface Sci. 73 (1978) 549.
[11] Y.D. Zheng, Y.H. Chang, B.D. McCombe, R.F.C. Farrow, T. Temofonte and F.A. Shirland, Appl. Phys. Letters 49 (1986) 1187.
[12] T.W. Kim, Y.H. Chang, Y.D. Zheng, A.A. Reeder, B.D. McCombe, R.F.C. Farrow, T. Temofonte, F.A. Shirland and A. Noreika, J. Vacuum Sci. Technol. B 5 (1987) 980.
[13] R.F.C. Farrow, D.S. Robertson, G.M. Williams, A.G. Cullis, G.R. Jones, I.M. Young and P.N.J. Dennis, J. Crystal Growth 54 (1984) 707.
[14] S. Satoh and M. Kimata, J. Crystal Growth 95 (1989) 564.
[15] K.J. Mackey, D.R.T. Zahn, P.M.G. Allen, R.H. Williams, W. Richter and R.S. Williams, J. Vacuum Sci. Technol. B 5 (1987) 1233.
[16] O. Madelung, M. Schulz and H. Weiss, in: Landolt–Börnstein III/7b (Springer, Berlin, 1982).
[17] O. Madelung and M. Schulz, in: Landolt–Börnstein New Series III/22a (Springer, Berlin, 1987).
[18] D. Long and J.L. Schmit, in: Semiconductors and Semimetals, Vol. 5 (Academic Press, New York, 1970) p. 195.
[19] G. Bastard and J.A. Brum, IEEE J. Quantum Electron. QE-22 (1986) 1625.
[20] A. Sasaki and M. Kimata, 53rd Applied Physics Congr., Osaka, Sept. 1992.